

Optimization of cogging torque in interior permanent magnet synchronous motor using optimum magnet v-angle

Introduction. At present, the most important requirement in the field of electrical engineering is the better utilization of electrical power, due to its increasing demand and not-so-increasing availability. A permanent magnet synchronous motor (PMSM) is increasingly gaining popularity in various household and industrial applications because of its superior performance compared to conventional electrical motors. **Purpose.** PMSM is designed based on the selection of various design variables and optimized to fulfill the same. Being superiorly advantageous over other motors, PMSM has the major disadvantage of higher cogging torque. Higher cogging torque generates torque ripple in the PMSM motor leading to various problems like vibration, rotor stress, and noisy operation during starting and steady state. The designer should aim to reduce the cogging torque at the design stage itself for overall better performance. **Methods.** An interior rotor v-shaped web-type PMSM is designed and its performance analysis is carried out using finite element analysis (FEA). Magnet v-angle is optimized with the objective of cogging torque reduction. Performance comparison is carried out between the optimized motor and the initially designed motor with FEA. **Novelty.** Magnet v-angle analysis is performed on the same keeping all other parameters constant, to obtain minimum cogging torque. The proposed method is practically viable as it does not incur extra costs and manufacturing complexity. **Practical value.** It is observed that the magnet v-angle is an effective technique in the reduction of cogging torque. Cogging torque is reduced from 0.554 N-m to 0.452 N-m with the application of the magnet v-angle optimization technique. References 19, tables 2, figures 10.

Key words: cogging torque, finite element analysis, interior v-shape web, magnet spread angle, magnet v-angle, permanent magnet synchronous motor.

Вступ. В даний час найважливішою вимогою в галузі електротехніки є найкраще використання електроенергії через зростаючу потребу в ній і не настільки зростаючу доступність. Синхронний двигун з постійними магнітами (СДПМ) набуває все більшої популярності в різних побутових та промислових застосуваннях завдяки своїм чудовим характеристикам у порівнянні зі звичайними електродвигунами. **Мета.** СДПМ, спроектований на основі вибору різних конструктивних змінних та оптимізований для їх виконання. Будучи чудовим у порівнянні з іншими двигунами, СДПМ має головний недолік: вищий крутний момент. Вищий крутний момент викликає пульсації крутного моменту в двигуні з постійними магнітами, що призводить до різних проблем, таких як вібрація, напруга ротора і шумна робота під час запуску і режиму. Проективальник повинен прагнути зменшити крутний момент зубчастого колеса на стадії проектування для підвищення загальної продуктивності. **Методи.** Розроблено СДПМ з внутрішнім ротором v-подібної форми та стрижневого типу, та аналіз його характеристик виконаний з використанням аналізу методом скінчених елементів (FEA). Кут v-подібного магніту оптимізовано з метою зниження зубчастого моменту. Порівняння продуктивності здійснюється між оптимізованим двигуном та двигуном, спочатку спроектованим за допомогою FEA. **Новизна.** Аналіз кута v-подібного магніту виконується таким же чином, зберігаючи решту всіх параметрів постійними, щоб отримати мінімальний зубчастий крутний момент. Запропонований спосіб практично життєздатний, оскільки не вимагає додаткових витрат та складності виготовлення. **Практична цінність.** Помічено, що v-подібний кут магніту є ефективним способом зниження зубчастого моменту. Зубчастий крутний момент зменшений з 0,554 Н·м до 0,452 Н·м за рахунок застосування методу оптимізації v-подібного кута магніту. Бібл. 19, табл. 2, рис. 10.

Ключові слова: крутний момент зубчастої передачі, аналіз методом скінчених елементів, внутрішнє v-подібне полотно, кут розкриття магніту, v-подібний кут магніту, синхронний двигун із постійними магнітами.

1. Introduction. The permanent magnet synchronous motor (PMSM) is increasingly gaining popularity in recent times because of its stellar performance with its smaller size. The moment of inertia and the dynamic response time is reduced due to its lesser size. It also turns out to be beneficial when there are spatial limitations. Its initial cost is higher compared to the induction motor, but thanks to its superior performance, its extra cost is paid back within just some time. It was developed keeping in view the elimination of synchronous machine exciters, which eventually decreases field winding losses and enhances performance and thermal conditions [1, 2]. Based on the magnet location, the two most common rotor configurations available for PMSM are surface permanent magnet (SPM) and interior permanent magnet (IPM). Among both of these, IPM beats SPM in terms of advantages. Because of the interior configuration of the magnets, they can be easily mounted in grooves, without the use of any binding material, which simplifies the manufacturing process and increases stability. As the magnets are not close to the air gap, the possibilities for demagnetization are also minimized. The increased saliency ratio also adds to the reluctance torque, which further enhances the average torque [3].

However, the concern with this motor is the cogging torque. It is an undesirable phenomenon. Cogging torque

is inherent in permanent magnet motors due to the presence of a permanent magnet and slotted stator. Cogging torque is the result of the interaction of magnetomotive force harmonics and air gap permeance harmonics. It degrades the motor performance and adds instability to the shaft movement, rendering the motion shaky. So, this unnecessary torque has to be reduced in torque-sensitive applications like traction, robotics, etc. The cogging torque can be minimized by choosing the appropriate magnet length. The equation involving optimum magnet length and slot pitch is given. By shifting the pole pairs, and creating an asymmetric distribution of the magnet pole, further reduction is also possible [4]. The same equation is improved, taking into account, the effects of the rotor curvature [5]. But the approach involves changes in the design of the rotor. The probability of asymmetry in flux distribution also exists. Another solution is to reduce the cogging torque by determining the optimal ratio of pole arc to pole pitch using no. of slots, no. of poles, and the goodness factor [6]. Simulations as well as experimental methods were used to validate the approach [7]. A novel approach consisting of torque ripple modeling and its use of the genetic algorithm to minimize cogging torque is also

presented [8]. The parameters needed as well as the calculations performed are more in this method. It's quite time-consuming. It also does not provide an angular spread of the magnets relative to the center of the rotor. Thus, magnet placement in an interior-type rotor has not yet been specified. The cogging torque can be minimized using skewing techniques. Recent developments also suggest step skewing of the rotor in which the rotor is axially skewed [3, 9]. V-shape skewing is also implemented in which, the skew is added in a v-shape to the axial rotor length [10]. But these are very complicated, exhaustive, and time-consuming approaches. Various rotor skewing techniques are compared for the generation of cogging torque, excitation torque ripple, average torque, and axial force [11]. The opening width of the slot and the shape of the magnet edge can also have an impact on the cogging torque [12].

Various types of rotor geometries are used for the flux barrier synchronous reluctance motor. The equation is given for the determination of the angular spread of flux barriers. It can also be used in the case of v-shape web type PMSM, as the magnet spread, because the principle behind the equation is the reduction of torque ripple by employing uniformity of reluctance only [13]. An approach to minimizing cogging torque using flux barriers is also presented [14]. The design of concentrated wound interior permanent magnet synchronous motor (IPMSM) with symmetrically positioned flux barriers to address smaller sensorless operating regions and significant torque ripples is proposed [15]. The Machaon structure having flux barriers, ending at some specific angles is also introduced, which can improve the cogging torque profile. The Taguchi method has been employed for shape design optimization [16]. The axial pole shaping of IPM machines to reduce the cogging torque as well as to obtain uniform distribution of flux density all over the surface is presented [17]. A hybrid rotor design, consisting of both circumferential as well as radial magnets, and having consequent rotor poles are also introduced to achieve an optimum synchronous performance of the motor [18]. But, the difficulties and expenses of manufacturing such kinds of rotors are very significant. Keeping uniformity and symmetry needs to be utmost considered.

So, in all the previous developments, it is either time-consuming and involves indirect calculations (in the case of the equation for optimum magnet length or optimum pole arc to pole pitch ratio or genetic algorithm using torque ripple modeling) or complicated and involves constructional changes (in the case of skewing), or affected by complexity and expenditure (in the case of axial pole shaping or step skewing). The v-angle is one of the major factors that influence the performance of IPMSM. The v-angle variation technique is straightforward, practically implantable hence suitable for the mass production of IPMSM. The proposed technique is more viable where cogging torque has relatively less effect on vibration and losses. Therefore, an approach is presented here, to find out the optimum magnet placement for cogging torque minimization.

The advantages of a PMSM are explained in section 1. The harmful impact of cogging torque and the limitations of its reduction techniques invented to date are also mentioned. Section 2 focuses on designing a PMSM. In section 3, the finite element analysis (FEA) of the same is carried out and different performance characteristics such

as cogging torque profile and torque-angle profile are analyzed. In section 4, the optimization of the designed motor is carried out for the magnet v-angle. The plot of the variation of cogging torque with respect to the magnet v-angle is also analyzed. From the attained results, the optimum magnet v-angle is found. The cogging torque, average torque, back electromotive force (EMF) spectrum, back EMF profile, and flux density plot are compared for both initial as well as the optimized model and the discussion of the same is carried out in section 5. In section 6, the conclusion from the exercise is drawn.

2. Design of PMSM. Owing to the many advantages of IPM over SPM, as evident from Section 1, IPM is selected for research purposes. Figure 1 shows the illustrative figure of the same which can help to understand terminology better. Figure 2 is the magnified view of the same.

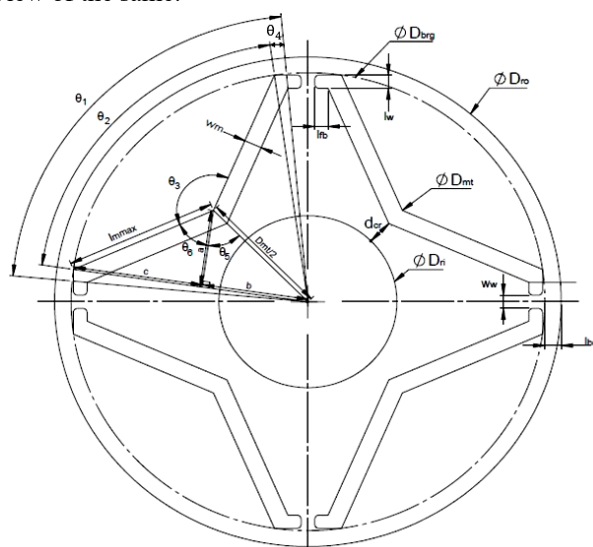


Fig. 1. Illustrative figure of interior v-shaped web type PMSM

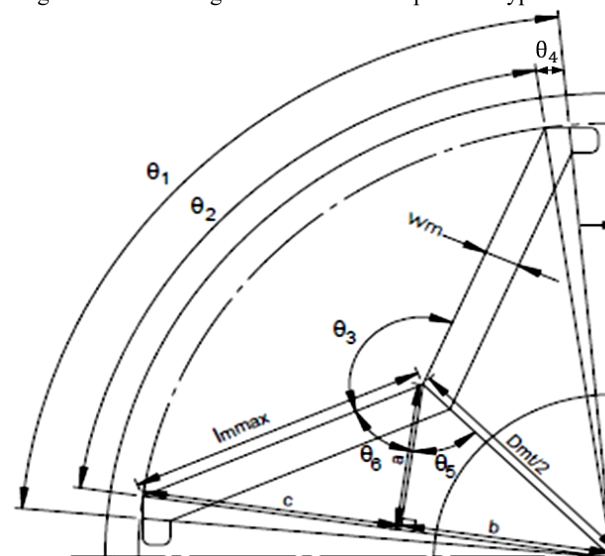


Fig. 2. Magnified view of Fig. 1

There are two magnet angles in the design of IPMSM. The first one is the magnet spread angle. This is known as the angular spread of a magnet pole in relation to the center of the rotor. This angle is shown as θ_1 in Fig. 1, 2. The other one is magnet v-angle, which is defined as the angular spread of a magnet pole in relation to the pole center. This angle is shown as θ_3 in Fig. 1, 2. Magnet

spread angle at the magnet top is θ_2 and the offset angle due to magnet thickness is θ_4 as shown in Fig. 1, 2.

PMSM of rating 4 kW, 415 V, 3-phase, and 50 Hz is designed. Necessary assumptions for specific magnetic loading, specific electric loading, number of poles, number of stator slots, aspect ratio, conductor packing factor, current density, tooth flux density, etc. are made. The design outcomes of this design are shown in Table 1.

Table 1
Design outcomes

Parameter	Value
Stator outer diameter D_o , mm	175
Stator inner diameter D , mm	120
Rotor outer diameter D_{ro} , mm	118
Core length L , mm	150
No. of stator slots S_s	36
Magnet width W_m , mm	5
Slot pitch λ , mm	10.46
Magnet spread angle θ_1	72°
Magnet v-angle θ_3	125°
Magnet length l_{max} , mm	33
Air gap thickness l_g , mm	0.5
Permanent magnet material	N38SH
Core material	M530-50A

3. FEA of the designed machine. The FEA of the designed machine is carried out using commercially available FEA software for design validation. Performance characteristics exhibited by this machine are observed, such as the cogging torque profile and torque-angle profile.

A two-dimensional (2D) finite element model of the designed machine is shown in Fig. 3.

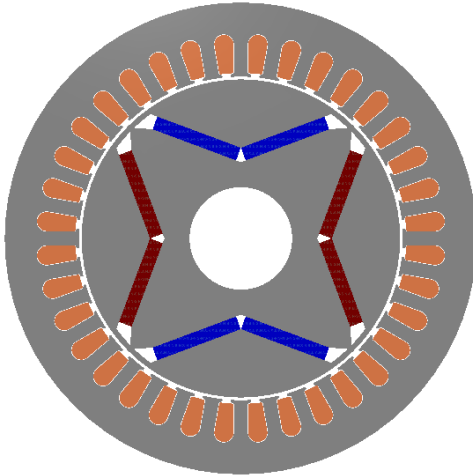


Fig. 3. 2D finite element model of the designed IPMSM

The dimensions to create this model are as per the analytical design. Each pole of the v-shape IPMSM consists of two magnet segments, to make v-shape poles. For different parts of the motor, appropriate materials are used. Figure 4 reveals that the peak cogging torque is 0.554 N-m. The cogging torque profile can be shown for one slot pitch only because of its repetitive nature for each slot pitch. Figure 5 dictates the variation of torque with respect to angular rotation. The maximum and minimum values are 36.1 N-m and 22.3 N-m respectively.

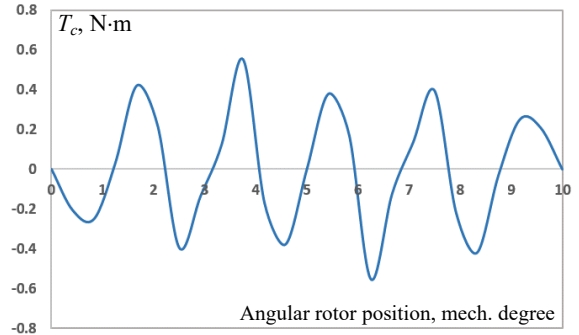


Fig. 4. Cogging torque profile

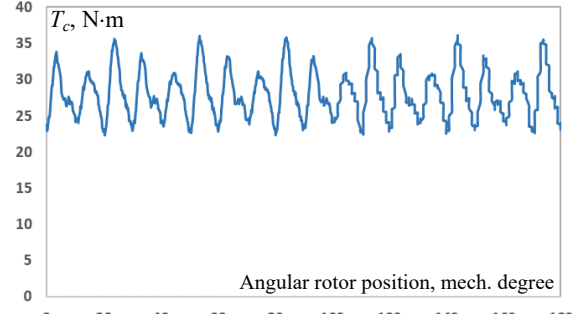


Fig. 5. Torque-angle profile

4. Optimization of the designed machine. As described earlier, cogging torque is an unwanted phenomenon. Therefore, it is necessary to reduce this torque. There is some specific relationship between cogging torque and reluctance variations. When the reluctance variation with respect to angular displacement increases, the cogging torque also increases. An equation is stated in [19], which describes this relationship as:

$$T_c = -\frac{1}{2} \cdot \Phi_g^2 \cdot \frac{dR}{d\theta}, \quad (1)$$

where T_c is the cogging torque; Φ_g is the air-gap flux; R is the reluctance of air-gap; θ is the angular displacement of the rotor.

As per the equation, the cogging torque can be reduced if the reluctance is made as uniformly as possible. This torque is the result of harmonic components present in the torque harmonic spectrum. So, it can also be represented in the Fourier series form, as mentioned in [8]:

$$T_c = \sum_{k=1}^{\infty} T_{ck} \cdot \sin(k \cdot \theta + \phi_k^c), \quad (2)$$

where T_{ck} is the magnitude of k^{th} cogging torque harmonic; k is the integer; ϕ_k^c is the phase angle of k^{th} cogging torque harmonic.

In this section, the cogging torque is optimized. The effort is made to achieve minimum cogging torque using magnet v-angle optimization. The magnet v-angle is changed and its effects on cogging torque are observed. During this entire optimization process, magnet volume, magnet length, magnet width, magnet spread angle, winding design, and slot dimensions have been kept constant.

Magnet v-angle is varied from 121° to 149° , above and below which the design fails to keep magnet dimensions constant due to geometrical constraints. During the entire process, the magnet spread angle is kept constant at the initial value of 72° . To achieve this, the magnet v-angle is increased by pushing the magnet segments away from the shaft. The geometrical constraint is that the original magnet length has to be retained while

pushing it upwards. This becomes necessary as, when the magnets are pushed upwards, the maximum allowed length (l_{max} in Fig. 2), which the geometry can afford, reduces. At one point, it reaches the boundary, and further increment of magnet v-angle becomes impossible. The results of this analysis are shown in Fig. 6.

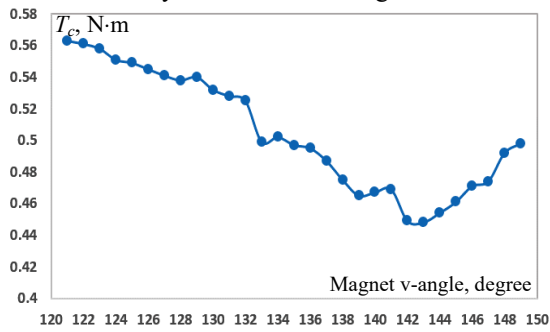


Fig. 6. Cogging torque vs. magnet v-angle

The figure dictates that the cogging torque reduces from 121° to 143° and then starts increasing. At 143° , the cogging torque is minimum. On both sides of 143° , it is increasing. So, this angle can be said as the optimum magnet v-angle for this design.

5. Result table and observations. FEA is carried out to obtain the peak cogging torque of the initial design and optimized design. The cogging torque period obtained for the designed 4 kW IPMSM is 10° mechanical. Cogging torque waveform period can be calculated as:

$$\theta_{cog-period} = \frac{360^\circ}{LCM(N_p, N_s)}, \quad (3)$$

where N_p is the number of poles; N_s is the number of stator slots; LCM is the least common multiplier.

Figure 7 shows the comparison of cogging torque profile for both, the initial as well as the optimized models. The peak cogging torque reduces from 0.554 N.m to 0.452 N.m.

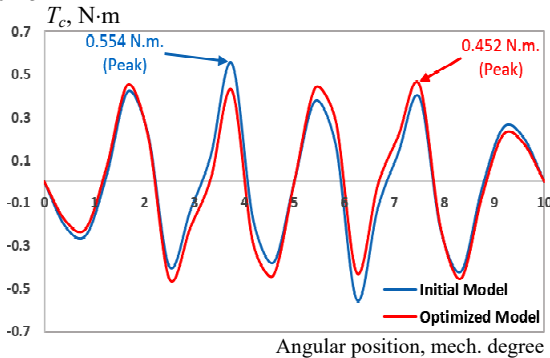


Fig. 7. Cogging torque profile of initial and optimized model

The performance comparison of the initial design and the optimized design is shown in Table 2.

Table 2

Comparison of initial and optimized design

Design	Cogging torque, N.m	Average torque, N.m
Initial	0.554	28
Optimized	0.452	28.2
Change, %	-18.41	0.71

Compared to the initial design, the optimized model shows an 18.41 % reduction in cogging torque and a 0.71 % increase in average torque. The back EMF profile comparison for the initial model, optimized model, and model having skewing of rotor poles is shown in Fig. 8.

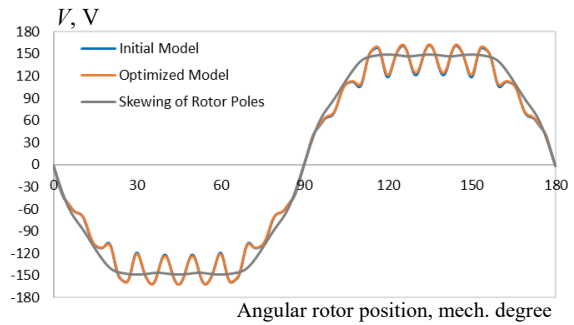


Fig. 8. Comparison of back EMF profiles of different models

It is evident from the same that there isn't much difference in the back EMF profile of the initial and optimized models. Both are looking almost similar to each other. It is analyzed that the back EMF profile obtained with a skewed rotor is smooth without any dips. Skewing is a known method to reduce cogging torque. However, there are some well-known disadvantages of skewing as well. For instance, the skewing of rotor magnets results in more axial thrust, more flux leakage, and a low winding factor. The skewed rotor of PM machines normally requires a magnet with a specific shape which complicates the design and increases the manufacturing difficulty as well as the cost. Skewing makes the rotor mechanically weak also. Skewing imposes limitations in mass production due to low manufacturability.

Figure 9 shows the comparison of the back EMF harmonics spectrum. Again, there isn't any appreciable change in the spectrum. The fundamental component of the back EMF is increased by 1 V. This slight increment has contributed to the minor increment of average torque achievable from the design. It is observed that after optimization, the even-order harmonics are eliminated and the other odd-order harmonics are decreased. The total harmonic distortions (THD) of the back EMF spectrum are also reduced slightly from 5.13 % to 5.04 % due to this spectrum improvement.

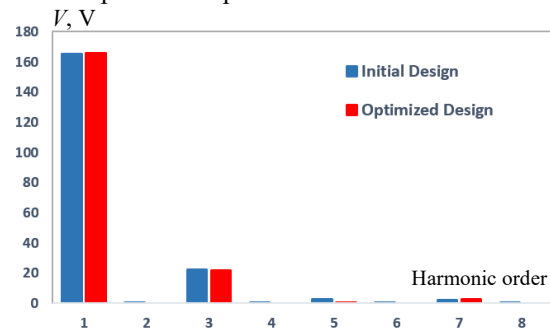


Fig. 9. Back EMF harmonic spectrum of the initial and optimized model

Figure 10 shows the flux density plot of both, the initial as well as the optimized models. In both cases, flux density at all parts is the same as that of the analytical design.

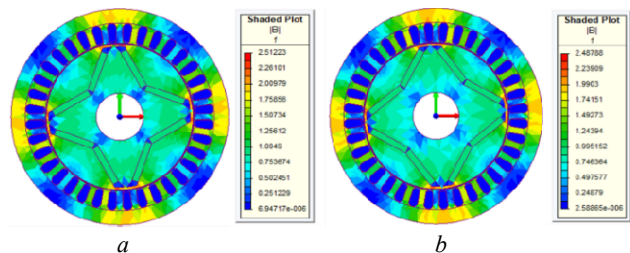


Fig. 10. Flux density plot of initial model (a) and optimized model (b)

From all these observations it can be said that the magnet v-angle has a major impact on cogging torque of the PMSM. It also has some minor impact on average torque, back EMF spectrum, and THD. Only by changing the placement of the magnet, cogging torque can be reduced. There is no need to change any other parameters or any other structural modifications required, which makes this technique practically viable and implementable, as it will not increase the complexity or initial cost of the motor. This is the novelty of the proposed methodology.

The reason behind this behavior can be stated as the uniformity of reluctance, at all times. As it is well-known, the cogging torque is the outcome of non-uniform reluctance distribution offered to magnet flux. But if we place the magnet such that, it faces nearly equal reluctance at all times, during the rotor rotation, it will face minimum reluctance, eventually resulting in minimum cogging torque.

6. Conclusions. The design of a permanent magnet synchronous motor and its finite element analysis is conducted for performance analysis. This initial design is considered a reference for further comparative performance analysis. Design optimization is performed with the objective of cogging torque minimization by optimization of magnet v-angle, and keeping all other dimensions constant. From the results obtained, it is analyzed that the magnet v-angle has a major impact on cogging torque. The cogging torque is reduced up to 18.41 % compared to the reference design. In addition to that, the average torque is increased by 0.71 % and the total harmonic distortions of back electromotive force reduces from 5.13 % to 5.04 % by application of magnet v-angle optimization.

Conflict of interest. The authors declare that they have no conflicts of interest.

REFERENCES

- Pillay P., Krishnan R. Application characteristics of permanent magnet synchronous and brushless DC motors for servo drives. *IEEE Transactions on Industry Applications*, 1991, vol. 27, no. 5, pp. 986-996. doi: <https://doi.org/10.1109/28.90357>.
- Panchal T.H., Patel A.N., Patel R.M. Reduction of cogging torque of radial flux permanent magnet brushless DC motor by magnet shifting technique. *Electrical Engineering & Electromechanics*, 2022, no. 3, pp. 15-20. doi: <https://doi.org/10.20998/2074-272X.2022.3.03>.
- Ge X., Zhu Z.Q., Kemp G., Moule D., Williams C. Optimal Step-Skew Methods for Cogging Torque Reduction Accounting for Three-Dimensional Effect of Interior Permanent Magnet Machines. *IEEE Transactions on Energy Conversion*, 2017, vol. 32, no. 1, pp. 222-232. doi: <https://doi.org/10.1109/TEC.2016.2620476>.
- Touzhu Li, Slemon G. Reduction of cogging torque in permanent magnet motors. *IEEE Transactions on Magnetics*, 1988, vol. 24, no. 6, pp. 2901-2903. doi: <https://doi.org/10.1109/20.92282>.
- Ishikawa T., Slemon G.R. A method of reducing ripple torque in permanent magnet motors without skewing. *IEEE Transactions on Magnetics*, 1993, vol. 29, no. 2, pp. 2028-2031. doi: <https://doi.org/10.1109/20.250808>.
- Zhu Z.Q., Howe D. Influence of design parameters on cogging torque in permanent magnet machines. *IEEE Transactions on Energy Conversion*, 2000, vol. 15, no. 4, pp. 407-412. doi: <https://doi.org/10.1109/60.900501>.
- Zhu Q., Ruangsinchaiwanich S., Schofield N., Howe D. Reduction of cogging torque in interior-magnet brushless machines. *IEEE Transactions on Magnetics*, 2003, vol. 39, no. 5, pp. 3238-3240. doi: <https://doi.org/10.1109/TMAG.2003.816733>.
- Lai C., Feng G., Iyer K.L.V., Mukherjee K., Kar N.C. Genetic Algorithm-Based Current Optimization for Torque Ripple Reduction of Interior PMSMs. *IEEE Transactions on Industry Applications*, 2017, vol. 53, no. 5, pp. 4493-4503. doi: <https://doi.org/10.1109/TIA.2017.2704063>.
- Luu P.T., Lee J.-Y., Hwang W., Woo B.-C. Cogging Torque Reduction Technique by Considering Step-Skew Rotor in Permanent Magnet Synchronous Motor. *2018 21st International Conference on Electrical Machines and Systems (ICEMS)*, 2018, pp. 219-223. doi: <https://doi.org/10.23919/ICEMS.2018.8549086>.
- Park G.-J., Kim Y.-J., Jung S.-Y. Design of IPMSM Applying V-Shape Skew Considering Axial Force Distribution and Performance Characteristics According to the Rotating Direction. *IEEE Transactions on Applied Superconductivity*, 2016, vol. 26, no. 4, pp. 1-5. doi: <https://doi.org/10.1109/TASC.2016.2543267>.
- Jiang J.W., Bilgin B., Yang Y., Sathyan A., Dadkhah H., Emadi A. Rotor skew pattern design and optimisation for cogging torque reduction. *IET Electrical Systems in Transportation*, 2016, vol. 6, no. 2, pp. 126-135. doi: <https://doi.org/10.1049/iet-est.2015.0021>.
- Nur T., Mulyadi M. Improve cogging torque method in inset-permanent magnet synchronous machine. *2018 IEEE International Conference on Applied System Invention (ICASI)*, 2018, pp. 1211-1213. doi: <https://doi.org/10.1109/ICASI.2018.8394506>.
- Jae Yoon Oh, Dal Ho Jung. *Flux Barrier Synchronous Reluctance Motor*. USA Patent no. 6239526B1, May 29, 2001.
- Kawaguchi Y., Sato T., Miki I., Nakamura M. A reduction method of cogging torque for IPMSM. *2005 International Conference on Electrical Machines and Systems*, 2005, vol. 1, pp. 248-250. doi: <https://doi.org/10.1109/ICEMS.2005.202522>.
- Kano Y. Sensorless-oriented design of IPMSM. *2014 International Power Electronics Conference (IPEC-Hiroshima 2014 - ECCE ASIA)*, 2014, pp. 2457-2464. doi: <https://doi.org/10.1109/IPEC.2014.6869934>.
- Rahimi Monjezi S., Kiyomarsi A., Mirzaei Dehkordi B., Sabahi M.-F., Vafaie M.-H. Shape Design Optimization of Interior Permanent-Magnet Synchronous Motor with Machaon Flux Barriers for Reduction of Torque Pulsation. *Electric Power Components and Systems*, 2016, vol. 44, no. 19, pp. 2212-2223. doi: <https://doi.org/10.1080/15325008.2016.1199611>.
- Du Z.S., Lipo T.A. Reducing Torque Ripple Using Axial Pole Shaping in Interior Permanent Magnet Machines. *IEEE Transactions on Industry Applications*, 2020, vol. 56, no. 1, pp. 148-157. doi: <https://doi.org/10.1109/TIA.2019.2946237>.
- Ugale R.T., Chaudhari B.N., Baka S., Pramanik A. A Hybrid Interior Rotor High-performance Line Start Permanent Magnet Synchronous Motor. *Electric Power Components and Systems*, 2014, vol. 42, no. 9, pp. 901-913. doi: <https://doi.org/10.1080/15325008.2014.903539>.
- Hanselman D.C. *Brushless Permanent Magnet Motor Design*. Magna Physics Publ., Ohio, 2006. 411 p.

Received 19.10.2022

Accepted 27.06.2023

Published 02.11.2023

A.N. Patel¹, PhD, Associate Professor,
P.J. Doshi², Traction Control Software Engineer,
S.C. Mahagoakar³, R&D Group Manager,
T.H. Panchal¹, PhD, Assistant Professor,

¹ Department of Electrical Engineering, Institute of Technology, Nirma University, Ahmedabad, Gujarat, India,
e-mail: amit.patel@nirmauni.ac.in;

tejas.panchal@nirmauni.ac.in (Corresponding Author)

² Alstom Transport India Ltd., Bangalore, Karnataka, India,
e-mail: 18meep03@nirmauni.ac.in

³ Rotomotive Powerdrive India Limited, Anand, Gujarat, India,
e-mail: s.mahagoakar@rotomotive.com

How to cite this article:

Patel A.N., Doshi P.J., Mahagoakar S.C., Panchal T.H. Optimization of cogging torque in interior permanent magnet synchronous motor using optimum magnet v-angle. *Electrical Engineering & Electromechanics*, 2023, no. 6, pp. 16-20. doi: <https://doi.org/10.20998/2074-272X.2023.6.03>